physica status solidi b
www.pss-b.com
basic solid state physics

Current-carrying capacity of semiconducting carbon nanotubes

Yung-Fu Chen and **Michael S. Fuhrer**

Department of Physics and Center for Superconductivity Research, University of Maryland, College Park, MD 20742-4111, USA

Received 20 April 2006, revised 28 June 2006, accepted 9 August 2006
Published online 2 October 2006

PACS 72.10.Di, 72.20.Ht, 73.40.Sx, 73.63.Fg

A simple Boltzmann-equation model for charge transport in semiconducting single-walled carbon nanotubes (s-SWNTs) is developed with two adjustable parameters, the acoustic and optical phonon scattering lengths. The model predicts velocity saturation rather than current saturation in s-SWNTs at high bias, in agreement with a recent experiment. At moderate densities, the model predicts currents in s-SWNTs exceeding 25 μA, the limiting current in long metallic single-walled carbon nanotubes.

phys. stat. sol. (b) **243**, No. 13, 3403–3407 (2006) / **DOI** 10.1002/pssb.200669170

WILEY-VCH

Original Paper

phys. stat. sol. (b) **243**, No. 13, 3403–3407 (2006) / **DOI** 10.1002/pssb.200669170

Current-carrying capacity of semiconducting carbon nanotubes

Yung-Fu Chen and **Michael S. Fuhrer***

Department of Physics and Center for Superconductivity Research, University of Maryland, College Park, MD 20742-4111, USA

Received 20 April 2006, revised 28 June 2006, accepted 9 August 2006
Published online 2 October 2006

PACS 72.10.Di, 72.20.Ht, 73.40.Sx, 73.63.Fg

A simple Boltzmann-equation model for charge transport in semiconducting single-walled carbon nanotubes (s-SWNTs) is developed with two adjustable parameters, the acoustic and optical phonon scattering lengths. The model predicts velocity saturation rather than current saturation in s-SWNTs at high bias, in agreement with a recent experiment. At moderate densities, the model predicts currents in s-SWNTs exceeding 25 μA, the limiting current in long metallic single-walled carbon nanotubes.

1 Introduction

The ultimate current-carrying capacity in carbon nanotubes is of great scientific [1–5] and technological interest [6, 7]. Metallic single-walled carbon nanotubes (m-SWNTs) have been shown to carry currents of 25 μA at high electric field [1], corresponding to current densities of $\sim 10^9$ A/cm^2, orders of magnitude larger than the typical thresholds for failure in metal wires due to electromigration [8]. The current limit in m-SWNTs can be understood as a result of their one-dimensional (1D) band structure: zone-boundary phonon scattering at $E_{zb} \approx 160$ meV limits the disequilibration of the quasi-Fermi levels for left- and right-moving carriers to $\sim E_{zb}$, and thus the current to $2G_0(E_{zb}/e) \approx 25$ μA, where G_0 is the quantum of conductance, 2 represents the number of 1D subbands in the m-SWNT, and e is the electronic charge. A Boltzmann-transport model which included only two scattering lengths for acoustic (elastic) and zone-boundary (160 meV) phonon scattering in m-SWNTs verified this expectation, and reproduced the experimental current-voltage (I–V) data and 25 μA current saturation [1].

Here we perform a similar Boltzmann-transport calculation for semiconducting SWNTs (s-SWNTs). In contrast to m-SWNTs, the current in s-SWNTs may significantly exceed 25 μA. We find that the electric-field-dependent velocity shows velocity saturation, with a saturation velocity v_{sat} which varies much less strongly with carrier concentration n than is would be expected for current saturation (i.e. $I = nev_{sat}$ predicts $v_{sat} \propto n^{-1}$). The results are in good agreement with recent experimental data on s-SWNT field-effect transistors in which currents up to 35 μA, and velocity saturation, rather than current saturation, were observed [9].

2 Boltzmann-transport study of carrier velocities in s-SWNTs

In solid state systems, the nonequilibrium distribution function g is used to describe the dynamics of the charge carriers (both electrons and holes). In carbon nanotubes, which are one-dimensional materials, the number of electrons at time t in the n-th subband in a phase space volume dx dk at point (x, k) is

* Corresponding author: e-mail: mfuhrer@umd.edu, Phone: +1 301 405 6143, Fax: +1 301 314 9527

$2g_n(x, k, t)\,\mathrm{d}x\,\mathrm{d}k/2\pi$ [10], where two is from the spin degeneracy of the electrons. In equilibrium, g_n is given by the Fermi distribution:

$$g_n(x,k,t) = f(E_n(k)) = \frac{1}{\mathrm{e}^{(E_n(k)-\mu)/k_\mathrm{B}T}+1}\,, \tag{1}$$

where $E_n(k)$ is the energy dispersion of the n-th subband, μ is the chemical potential, k_B is Boltzmann constant, T is the temperature. Here we only treat the first subband (and hence drop the subscript n at this point), and approximate the dispersion relation as hyperbolic: $E(k) = \sqrt{\Delta^2 + (\hbar v_\mathrm{F} k)^2}$, where $\Delta = 420$ meV-nm/d with d the s-SWNT diameter [11, 12], $v_\mathrm{F} = 9.3 \times 10^7$ cm/s is the Fermi velocity in graphene, and $\hbar$ is Planck's constant divided by 2π. Here we take d to be 2.1 nm such that $\Delta = 200$ meV.

When an applied electric field F is present, g deviates from Fermi distribution [10]. The dynamics of g is governed by Boltzmann equation:

$$v(k)\frac{\partial g(x,k,t)}{\partial x} + \frac{eF}{\hbar}\frac{\partial g(x,k,t)}{\partial k} + \frac{\partial g(x,k,t)}{\partial t} = \left(\frac{\mathrm{d}g}{\mathrm{d}t}\right)_{\text{collision}}\,, \tag{2}$$

where the right side of the Eq. (2) is the distribution change rate due to the collisions. In steady state, $\frac{\partial g(x,k,t)}{\partial t} = 0$, and further assuming no carrier density variation along x so that $\frac{\partial g(x,k,t)}{\partial x} = 0$, then

$$\frac{eF}{\hbar}\frac{\partial g(k)}{\partial k} = \left(\frac{\mathrm{d}g}{\mathrm{d}t}\right)_{\text{collision}}\,. \tag{3}$$

The collision term in the Boltzmann equation can be simply described by relaxation lengths if there are multiple sources of scattering:

$$\left(\frac{\mathrm{d}g}{\mathrm{d}t}\right)_{\text{collision}} = \sum_{\mathrm{s},k'} \frac{v(k)}{l_\mathrm{s}}\left((1-g(k))\,g(k') - g(k)\,(1-g(k'))\right), \tag{4}$$

where the first term in right side of Eq. (4) denotes the carriers scattering in to state k from state k', while the second term denotes the carriers scattering out from state k to state k', and s stands for different types of scattering transitions.

We approximate the electron–phonon scattering using two categories: nearly elastic scattering (corresponding to low energy acoustic phonons) and strongly inelastic scattering (optical and zone-boundary phonons); the scattering strengths are characterized by l_ac and l_op, respectively. Figure 1 shows approximate

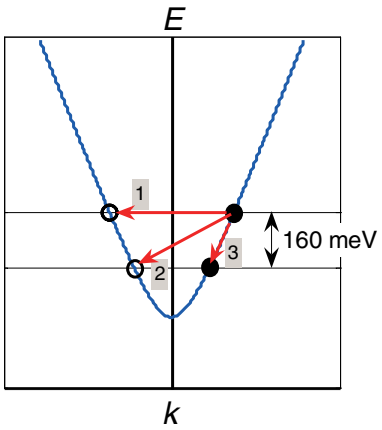

Fig. 1 (online colour at: www.pss-b.com) Approximate electron–phonon scattering transitions in a single band. The filled and empty circles indicate the states which are occupied and empty, respectively. The arrows indicate some possible scattering events. The scattering transitions toward empty states are permitted; however, the scattering transitions toward filled states are prohibited because of the exclusion principle.

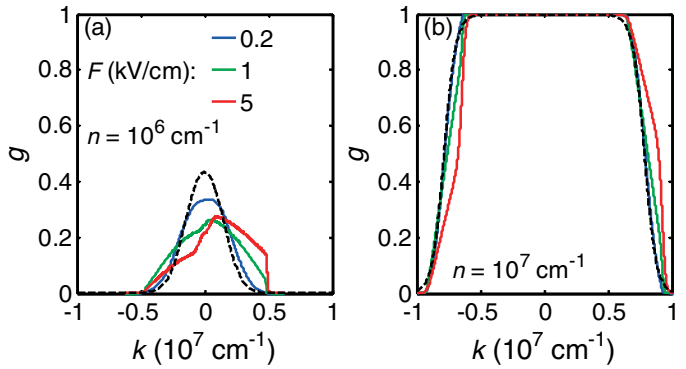

Fig. 2 (online colour at: www.pss-b.com) Nonequilibrium distribution function $g(k)$ under different F (a) at $n = 10^6$ cm^{-1}, and (b) at $n = 10^7$ cm^{-1}. The dashed curve represents the Fermi distribution at $T = 300$ K. The bandgap of the universal dispersion relation used in this calculation is 0.4 eV.

electron–phonon scattering transitions in a single band. The filled and empty circles indicate the states which are occupied and empty, respectively. The arrows indicate some possible scattering transitions. Arrow 1 indicates a nearly elastic electron–phonon scattering transition, while arrows 2 and 3 indicate inelastic electron–phonon scattering transitions. Because the optical phonon energies and zone-boundary phonon energies are all about 160 meV with small dispersion, the emission energy of phonons required by inelastic electron–phonon scattering is simply set at 160 meV (phonon absorption is not considered because the population of phonons of 160 meV is very small even at room temperature). The transitions 1 and 2 toward empty states are permitted; however, the transition 3 toward filled states is prohibited simply because of the exclusion principle.

By solving Eq. (3), the nonequilibrium distribution function $g(k)$ corresponding to each F is obtained. Figure 2 shows $g(k)$ at three different F. Note that the dashed curve represents the Fermi distribution at $T = 300$ K, which is symmetric with respect to $k = 0$. Under F the distribution has higher weight in one k direction than in the opposite, which causes a nonzero average carrier velocity (drift velocity); therefore nonzero current. As F increases, the asymmetry becomes more pronounced. $g(k)$ has a sharp decline at the point where the corresponding energy of the state is about 160 meV higher than the energy of the lowest available (empty) state when F is high. This occurs because once carriers have the energies

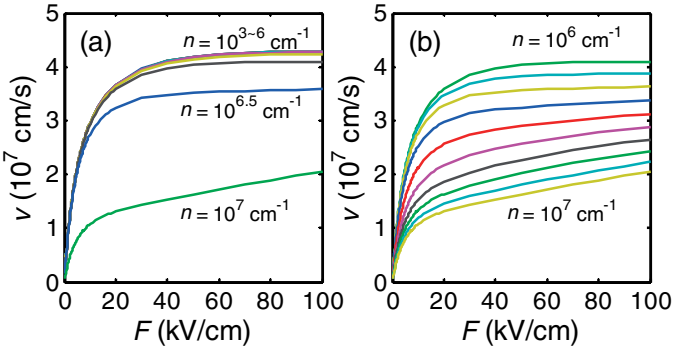

Fig. 3 (online colour at: www.pss-b.com) v vs. F at different carrier densities with density increasing (a) exponentially from 10^3 cm^{-1} to 10^7 cm^{-1} in $10^{0.5}$ cm^{-1} steps, and (b) linearly from 10^6 cm^{-1} to 10^7 cm^{-1} in 10^6 cm^{-1} steps. l_{ac} and l_{op} used for this calculation are 300 and 10 nm, respectively.

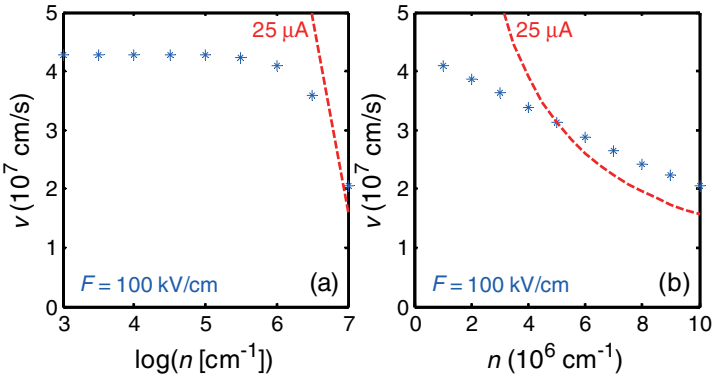

Fig. 4 (online colour at: www.pss-b.com) v at $F = 100$ kV/cm as a function of carrier density n (a) in logarithmic scale, and (b) in linear scale. The red dashed lines indicate the v-n relation corresponding to a current of 25 μA.

160 meV higher than the energy of the lowest available state, they start to emit phonons and relax to lower energy states. After obtaining $g(k)$ and then evaluating the average carrier velocity

$$v = \frac{\sum_k g(k)\, v(k)}{\sum_k g(k)}, \tag{5}$$

at many different F, the v-F relationship can be determined.

First, motivated by experiments in m-SWNTs [1–3], we choose values for the numerical calculation of $l_{ac} = 300$ nm and $l_{op} = 10$ nm. Figure 3 shows the average carrier velocity v as a function of applied electric field F at different carrier density n with density increasing (a) exponentially from 10^3 cm^{-1} to 10^7 cm^{-1} in $10^{0.5}$ cm^{-1} steps, and (b) linearly from 10^6 cm^{-1} to 10^7 cm^{-1} in 10^6 cm^{-1} steps. Note that a carrier density of 10^3 cm^{-1} is identical to one carrier in a 10 μm nanotube. In Fig. 3(a), the curves with low carrier densities collapse to a single curve with velocity-saturation like behavior. However, as the density increases beyond a threshold density $\sim 10^6$ cm^{-1}, the velocity decreases with increasing density. Although the velocity still seems to saturate at high F, the saturation velocity decreases monotonically with increasing density (see Fig. 3(b)). Similar velocity-saturation behavior for a single-carrier picture in multiple subbands was predicted by Perebeinos, et al. [13].

The blue star points in Fig. 4 show v at $F = 100$ kV/cm as a function of carrier density n (a) on a logarithmic scale, and (b) on a linear scale from the data in Fig. 3. The trend of the saturation velocity with respect to the carrier density is easily noticed. As discussed previously, the saturation velocity does not vary with the carrier density at low carrier densities, but falls nearly linearly at high carrier densities. If current saturation were obeyed, $I = nev$ predicts $v \propto n^{-1}$. This is a reasonable expectation when considering only a single valence and conduction subband (excluding inter-subband scattering) and very strong optical phonon scattering; here one might expect the current to saturate 25 μA at high electric fields as in m-SWNT, once the difference between quasi-Fermi levels for left- and right-moving carriers is 160 meV. The red dashed lines in Fig. 4 indicate the v-n relation corresponding to a current of 25 μA. In contrast to this expectation, the calculated (blue star) points are higher than the red dashed lines at high carrier densities and electric fields, indicating that the current is higher than 25 μA. Therefore, in our model, it is possible that the current can exceed 25 μA in s-SWNTs even though zone-boundary phonon emission is strong and only a single band is occupied.

3 Discussion and summary

Perebeinos, et al. [14] have calculated the carrier velocity in s-SWNTs as a function of carrier density and electric field, for different tube diameters and temperatures. They have found the average carrier velocity saturates at various velocities depending on carrier density. They have also found that below a critical density, n_c about 3.5 to 5.0×10^6 cm^{-1}, the velocity reaches a maximum and then experiences negative differential mobility with increasing field. Above n_c, the velocity increases with field strength with no apparent saturation, which is also seen in our numerical calculation for the lowest conduction band or highest valence band transport. It is interesting that our simple model reproduces many features of the more detailed calculations of [14]; this indicates that our model indeed captures the essential physics of scattering in s-SWNTs. The simplicity of our model should allow other researchers studying s-SWNT devices to perform facile calculations of the *v*-*F* relationship as a function of e.g. s-SWNT diameter, temperature, and l_{ac} and l_{op}.

Other studies have predicted negative differential conductance or negative differential mobility in s-SWNTs at high-bias transport [13, 15], which does not appear in our numerical study. One of the reasons is that for simplicity the electronic dispersion relation is approximated here by the hyperbolic universal dispersion relation [16], where the carrier velocity asymptotically approaches the Fermi velocity of graphene as energy increases. The universal dispersion relation has non-negative curvature, whereas the real electronic band structure has negative curvature at high energy. Therefore, as more and more carriers have very high energies, the average velocity decreases, causing negative differential conductance or negative differential mobility. Additionally, our calculation is restricted to a single subband; inter-subband transitions would tend to reduce the mobility at high carrier energies (high *F*).

In conclusion, our simplified Boltzmann calculation predicts the carriers in s-SWNTs experience velocity-saturation-like behavior with a saturation velocity about half of the graphene Fermi velocity at low carrier density, and decreasing monotonically with increasing density at high carrier density. The current exceeds 25 μA at experimentally-accessible fields and carrier densities, even in our simple single-band model.

Acknowledgements The authors are grateful for support from the NSF under grant DMR-01-02950, and the NSF-Materials Research Science and Engineering Center under Grant No. DMR-05-20471.

References

[1] Z. Yao et al., Phys. Rev. Lett. **84**, 2941 (2000).
[2] A. Javey et al., Phys. Rev. Lett. **92**, 106804 (2004).
[3] J. Y. Park et al., Nano Lett. **4**, 517 (2004).
[4] P. G. Collins et al., Phys. Rev. Lett. **86**, 3128 (2001).
[5] B. Bourlon et al., Phys. Rev. Lett. **92**, 026804 (2004).
[6] P. G. Collins et al., Science **292**, 706 (2001).
[7] B. Q. Wei et al., Appl. Phys. Lett. **79**, 1172 (2001).
[8] D. Young and A. Christou, IEEE Trans. Reliab. **43**, 186 (1994).
[9] Y. F. Chen and M. S. Fuhrer, Phys. Rev. Lett. **95**, 236803 (2005).
[10] N. W. Ashcroft and N. D. Mermin, Solid State Physics (Brooks/Cole, 1976).
[11] R. Saito et al., Physical properties of carbon nanotubes (Imperial College Press, 1998).
[12] A. G. Souza et al., Phys. Rev. B **63**, 241404 (2001).
[13] V. Perebeinos et al., Phys. Rev. Lett. **94**, 086802 (2005).
[14] V. Perebeinos et al., Nano Lett. **6**, 205 (2006).
[15] G. Pennington and N. Goldsman, Phys. Rev. B **68**, 045426 (2003).
[16] J. W. Mintmire and C. T. White, Phys. Rev. Lett. **81**, 2506 (1998).

